ARTIFICIAL INTELLIGENCE APPROACH TO PREDICTING GEODETIC POINT VELOCITY USING GNSS CAMPAIGN DATA (A CASE STUDY OF GHANA)

Paper No: 12376

Christian Kartey QUARCOO, Yao Yevenyo ZIGGAH (PhD.) and Bernard KUMI-BOATENG (Prof.), Ghana

Keywords: Geodetic point velocity 1, seismicity 2, crustal motion 3, RBFNN GRNN GMDH BPNN 4, artificial intelligence 5, etc.

SUMMARY

The frequent occurrence of disasters worldwide has incited the need for rigorous experimentation with techniques that would help mitigate risk, as these disasters result in countless loss of lives and properties, thus, increasing the economic expenditure of nations. Therefore the forecasting of a precise crustal movement is of great significant, not only to the geoscience community but the world at large. One way to understand crustal movement geodetically is by using Geodetic Point Velocity. The object of this research is to analyze the predictive capability of four Artificial Neural Network (ANN) models in predicting GPV in Ghana. Based on the observations of the 8 GNSS CORS in the southern part of Ghana, the velocity data derived was divided into two; 80% for training and 20% for testing and validation. First, the BPNN model was developed with 3 inputs, i.e. V_x, V_y and V_z, 50 hidden layers with their synaptic weights and 1 output layer. Afterwards, the remaining three models, GRNN, RBFNN and GMDH were trained and tested with the same dataset. Geocentric coordinates Xm, Ym and Zm with their respective Geodetic Point Velocities were used as inputs (V_X, V_Y, V_Z) for all the models. The performances of the models were assessed using root mean square error, mean absolute error, mean squared error and coefficient of determination. Based on the results obtained, it was found out that 3 out of the 4 proposed AI techniques were able to produce sound GPV predictions. However, the GMDH was suitable as it was able to predict the GPV precisely. This was selected based on the statistical approach for the evaluation of the prediction of the models. For instance, the other models could produce comparable results as their R^2 values were marginally different from that of the GMDH model which ranges between of 0.002 to 0.298.

1. INTRODUCTION

It is established that society faces a continuum of everyday risks to major disasters. Hence, it is a great concern that severe natural disasters (e.g., earthquakes, floods, and tsunamis) are generally infrequent but significantly impact society. For example, destructive earthquakes and other seismic risks greatly impacted various countries regarding loss of lives, economic losses and downtimes. (Songsore, 2006).

The practical application of science and engineering principles to developed economies through precise predictions of seismic activities has reduced the risk faced by earthquake-threatened cities of the developed world through Artificial Intelligence (AI). However, less can be said about developing countries, for instance, Ghana. It is worth noting that rapid advancements in AI have far-reaching ramifications for engineering practitioners and society as a whole.

AI has been applied in many engineering fields as well as geodesy for the determination and prediction of geo-seismic activities of the earth (Reiter *et al.*, 2010).
Recently, the use of AI in geodesy has been widely adopted as an alternative to the conventional methods of solving most geodetic problems. Notable areas of application include coordinate transformation (Ziggah *et al*., 2012; Ziggah *et al*., 2019; Ziggah *et al*., 2020, Gullu, 2010; Konakoğlu and Gökalp, 2016; ; Cakir and Konakoglu, 2019), geoid determination (Kavzoglu and Saka, 2005; Veronez, 2011; Erol and Erol, 2013; Cakir and Yilmaz, 2014), earth orientation parameter determination (Schuh, 2002; Wang, 2008; Liao, 2012), modelling ionospheric TEC (Cander, 1998; Maruyama, 2008; Akhoondzadeh, 2014; Inyurt and Sekertekin, 2019), gravity anomaly prediction (Tierra and De Freitas, 2005; Pereira, 2012), noise reduction in GNSS signals (Mosavi, 2006; Kaloop and Hu, 2015) and crustal movement (Laksari *et al*.,2012; Yilmaz and Gulu, 2014; Yilmaz, 2013; Argus, 2012; Razin and Mohammedzadeh, 2015; Tierra, 2016). It is important to note that this study is focused on crustal movement.

It is established that tidal forces from external bodies cause crustal movement within the earth. Hence, there is an increasing demand for precision and accuracy in crustal movement prediction for geodetic and survey measurements. Therefore, highly potent mathematical methods such as AI are needed to model and predict crustal movement. In effect, the impact of crustal movement on the earth's surface could be ascertained and proper mitigation measures be applied (Agnew, 2007). One way to understand the crustal movement geodetically is by using geodetic point velocity.

Therefore, estimating accurate geodetic point velocity is significant to geoscientific-based communities. Several researchers have investigated the velocity field determination in crustal movement (e.g., Demir and Acikgoz, 2000; Nocquet and Calais 2003; Hefty, 2008; Novotny and Kostelecky, 2008). In addition, the velocity information can be used to study plate boundary dynamics, seismic site characterization and deformation kinematics (e.g., McClusky, 2000; Hackl *et al*., 2009; Kanli, 2009; Perez-Pena, 2010; and Pinna, 2011). This study adopts an AI approach to develop a computational tool for predicting crustal movement.

1.1 Problem Statement

By the end of the 20th century, the primary data sources for understanding tectonic deformation were field fault surveys, satellite images and seismic moment tensor inversions (Avouac and Tapponnier, 1993; Ding, 1986). With the rapid development of modern space geodesy, geophysical phenomena such as tectonic movement, fault zones, earthquakes, landslides, volcanoes and other deformation activities are frequently determined using GPS/GNSS campaigns. Repeated observations from the GPS/GNSS provide velocity information with high precision and high spatiotemporal resolution (Wonnacott *et al*., 2011), hence resulting in the varying positioning of geodetic points over time evolution (Duman and Dogan, 2018).

GPS/GNSS derived velocity field has proven to be an effective source of information for determining the displacement of points in horizontal and vertical space. Its applications also span through but are not limited to the: determination of plate boundaries and their movements, displacement of geodetic points, crustal motion, geo-kinematic model, the magnitude of earthquakes, velocity of mass center and the surface of the earth, rotational rate and spatial density variations of the earth (Haukson, 2001; Hofman *et al*., 2006; Heildelberg, 2013 and Younis, 2019).

There has been a remarkable increase in modeling of geodetic point velocity that has been done over the years, particularly by scholars with the ability to predict the earth's seismicity and lithology over varying plates. Some of the notable empirical methods applied to model geodetic displacement and or deformation include Kriging, vector displacement, least squares collocation, linear propagation of errors, Quasi-Newton model, NUVEL model, triangulation method, dislocation model, Ferrell's Green functions and VEMOS (SIRGAS velocity model) (Tierra, 2016; Rinlin *et al.*, 2014; Zhou e*t al.*, 2010; Rizos e*t al.*, 2004; Liu *et al.*, 2011; Li *et al.*, 2015; Shen, 2004; Bock and Melgar, 2015 and Kahle *et al.*, 2006). However, these mentioned methods tend to be laborious due to the data acquisition method, length of observation and the computational challenges it presents. It also poses computationally intense calculations with sparse matrixes and is not easily scalable to global (Blewitt *et al*., 2013). For example, the vector displacement model describes velocity in 2/3-dimension axes in a pre-defined coordinate system and computes the displacement of points in 3 dimensions. Therefore, if there is a change in position, the velocities in X, Y and Z (Vx, Vy and Vz), which are functions of time (t), become a vector algebra and not scalar, hence presents a complex situation to handle when performing manual computation.

Currently, AI techniques and Global Navigation Satellite System (GNSS) Continuously Operating Reference Stations (CORS) data have been coupled for determining and monitoring crustal motion and are perhaps one of the most evident. For example, Yilmaz and Gullu (2011) evaluated the geodetic point velocities of five (5) stations in Turkey using Back propagation Neural Network (BPNN), Radial Basis Function Neural Network (RBFNN) and Kriging. It turned out that the BPNN point velocity estimation was better than the RBFNN and Kriging estimations in all geodetic networks. Similarly, Tierra (2016) proposed a strategy

to interpolate the geodetic point velocities using RBFNN and the empirical VEMOS09 model. The results demonstrated that RBFNN could interpolate better than the traditional VEMOS09 model. These mentioned studies have shown the capabilities of AI methods.

Although AI methods are generally more robust than traditional statistical regression methods, each method has limitations based on how much noise a model can tolerate in data. Furthermore, a specific AI method may be effective only for a particular task, and once the object of focus changes, prediction performance may intensely reduce (Li *et al*., 2019; Du *et al*., 2019).
It is established that the earth's plate moves at an average 25mm/year rate, however, no research has shown the share of local rates in the global average. Therefore, this research applied four AI methods: BPNN, RBFNN, Generalized Regression Neural Network (GRNN) and Group Method of Data Handling (GMDH) to predict local crustal movement within the southern part of Ghana. The key is to select the optimal AI method with higher generalizability that can correctly manage the non-linearity and high parallelism traits displayed by the varying velocity fields of the earth.

1.2 Study Area

The study area is Ghana; a West African country located between latitudes 4° 30´ N and 11° 00N and longitudes 3° W and 1° E. It is bordered on the North by Burkina Faso, Ivory Coast to the West, Togo to the East and The Gulf of Guinea of the Atlantic Ocean lies on the southern part of the country, forming a coastline of about 550 km long. Ghana covers a total land area of about 239,000km^2. Ghana's Geodetic Survey started as far back as June 1904 by the Governor of the then Gold Coast, Gordon Guggisberg, who made observation for latitude from a pillar in Accra with a zenith telescope, to 15 stars giving the final probable error of 0.360 2009).

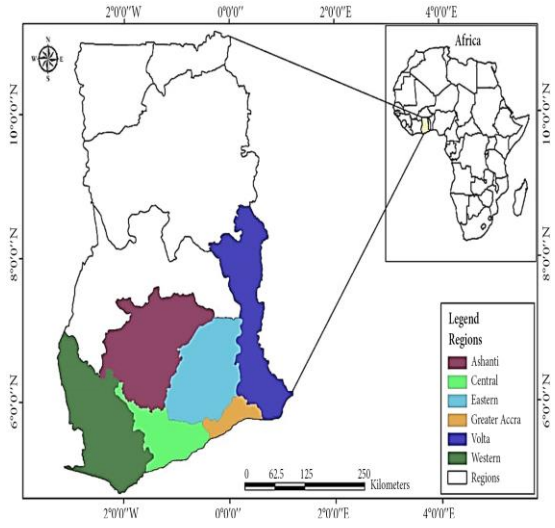

Figure 1: The Study Area Showing the Six Selected Regions of Ghana.

Ghana's framework diagram of Geodetic Network which is a blend of triangulation, traverses and precise levels, is covered with triangulation points with baselines of up to a maximum of about 55 miles and is controlled by three (3) measured bases; one base near Krobo Odumase in the Eastern Region, the second one is at Obuasi in Ashanti Region and a third at Laura in the Brong Ahafo Region (Poku-Gyamfi, 2009). The triangulation was mainly in the mountainous south, up to latitude 8º 20' N and parts of the Volta Basin; the northern regions and the coastal lowlands were covered with traverses. These were supplemented with secondary traverses and primary levels. Primary traverses are found along the coastal belt with the exception of less than 100 km stretch between Accra and Apam in the Central Region of Ghana which has triangulation points. This network was published by the Survey Department in 1970, and is what has been used to provide controls for mapping in the country.

The above description gives the researcher the advantage to undertake the research in Ghana, hence the study seeks to estimate and predict local crust movement for southern sector of Ghana.

1.3 Theoretical Framework

Konakoglu, (2020) on Prediction of geodetic point velocity using MLPNN, GRNN, and RBFNN models: a comparative study by using first the multi-layer perceptron neural network (MLPNN) model with two hidden layers and generalized regression neural network (GRNN) model was then applied for the first time. Afterwards, the radial basis function neural network (RBFNN) model was trained and tested with the same data. Latitude (φ) and longitude (λ) were utilized as inputs and the geodetic point velocities (V_X, V_Y, V_Z) as outputs to the MLPNN, GRNN, and RBFNN models. The performances of all ANN models were evaluated using root mean square error (RMSE), mean absolute error (MAE), and coefficient of determination (R2). The first investigation demonstrated that it was possible to predict the geodetic point velocities by using all the components as output parameters simultaneously. The other result is that all ANN models were able to predict the geodetic point velocity with satisfactory accuracy; however, the GRNN model provided better accuracy than the MLPNN and RBFNN models.

2. RESOURCES AND DATA USED

2.1 GNSS Data Description

Global Navigation Satellite System (GNSS) campaign data were obtained from the Eight (8) Continues Operation Reference Stations (CORS) established and controlled by the Licensed Surveyors Association of Ghana (LISAG).

It was established between the years of 2017 and 2019. In other words, the 8 CORS were not established the same year but all eight (8) became fully operational in January, 2019.

The GNSS receivers installed are the Leica GRX1200 series GNSS receivers with AS10 antennas.

The CORS is currently operating in the southern part of Ghana, i.e. Accra-Spintex, Akim-Oda, Winneba, Tarkwa, Koforidua, Tarkoradi, Kumasi and Ho as listed in the table below.

The data were obtained in Receiver Network Exchange (RINEX 3.0) Format with a mast/cutoff angle 13^{o} and of 30 seconds recording rate for 24hour session daily spanning 3 years which supersedes the minimum time interval (i.e. 1 year) one can analyze deformation rate using GNSS data.

Table 1. Stations from which GNSS data was used.

Stat.	Lat.(N)	Lon. (W)	Alt.(m)
LSA1	*5°38'01.254"*	*0°05'15.516"*	*75.57*
LSA2	*6°41'16.602"*	*1°37'30.818"*	*309.87*
LSA3	*5°17'51.709"*	*2°00'00.156"*	*108.27*
LSA4	*6°06'33.359"*	*0°18' 8.364"*	*222.38*
LSA5	*4°55'31.741"*	*1°46'26.643"*	*43.62*
LSA6	*5°21'38.166"*	*0°37'59.504"*	*44.90*
LSA7	*5°55'34.325"*	*0°59'11.021"*	*164.54*
LSA8	*6°36'33.322"*	*0°27'37.320"*	*230.49*

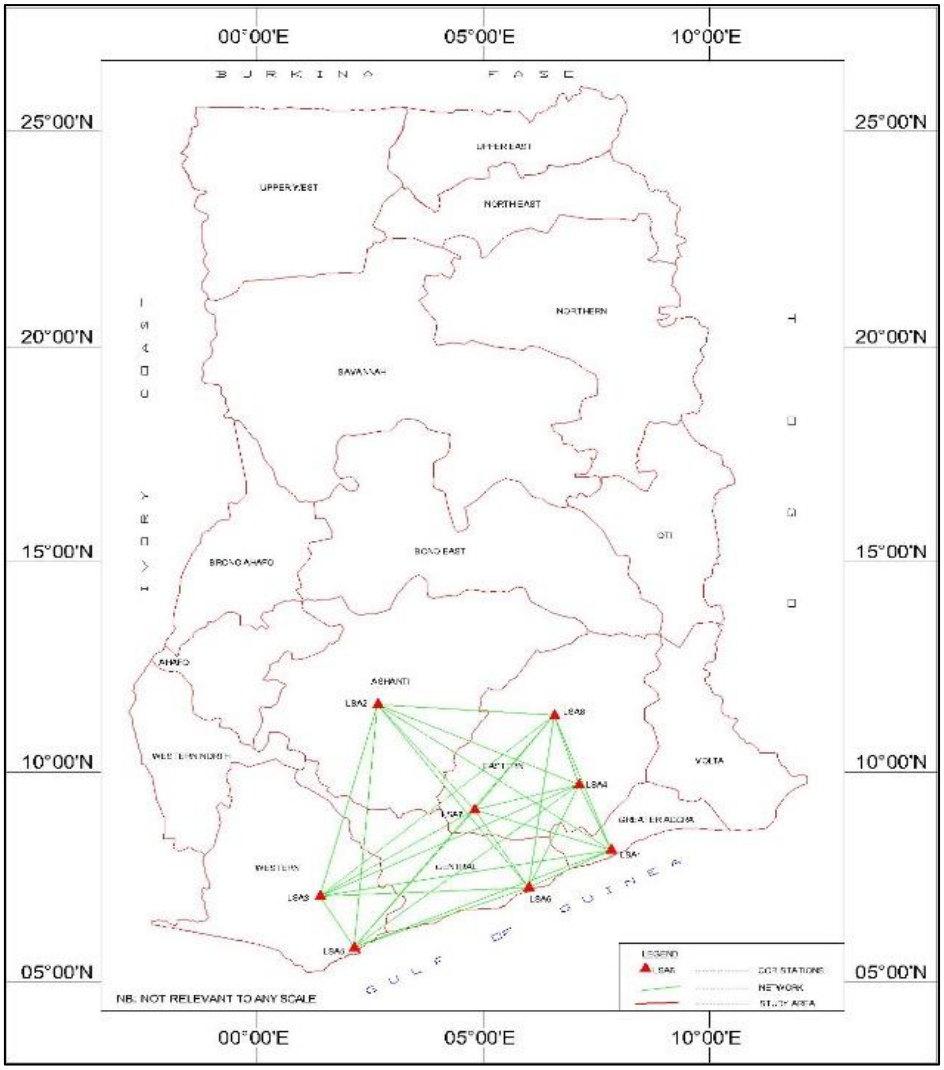

Figure 2. Map of the study area showing the network of the CORS

2.1.1 GNSS Data and post-processing

The Trimble Business Centre (TBC), developed by Trimble Geospatial was used to process the GNSS observation data.

In order to resolve the ambiguities of the baselines among the networks no station was assigned as Reference Station for the network to obtain the natural coordinates of the stations. Due to the size of data and the number of observation files the stations were processed on yearly basis to avoid excessive pressure on the processing software.

Since the program is based on relative positioning, the daily set of baselines were formed in a network adjustment involving all station for each day for the 3year period.

The datum chosen was WGS1984 with geographic cartesian coordinates Nm, Em and Zm and the tropospheric model used in the TBC processing was the Saastomoinen model since it is professed as the best model in GNSS signal processing for multi-frequency GNSS observations.
In all, there were 1070 station observations processed for the 8 stations and their respective coordinates derived during the study period.

2.2 Velocity data processing

2.2.1 Velocity data processing using GAMIT/GLOBK

GAMIT/GLOBK is a Linux-based operating system propriety software developed by Massachusetts Institute of Technology (MIT). It is scientific software used to process the GNSS data for geophysical analysis.
The "globk" refer loosely to the ensemble of programs collected in the ("Kalman filter") directory of the software distribution.
Globk is a *Kalman filter* whose primary purpose is to combine solutions from the processing of primary data from space-geodetic or terrestrial observations.
The Kalman filtering model is given as:'

$$\hat{X}_K = K_k \,.\, Z_k \, + (1 - K_k) \,.\, \hat{X}_{k-1} \tag{1}$$

Where **k**'s (superscripts) are states, k=1 means 1ms, k=2 means 2ms.

$\hat{X}_K$ is the estimate of the signal **x**.

Z_k is the measurement value.

K_k is called "**Kalman Gain.**"

and $\hat{X}_{k-1}$ is the estimate of the signal on the previous state.

2.3 Artificial Intelligence Techniques

This study applied four (4) Artificial Intelligence (AI) techniques to predict and evaluate the best model for Geodetic Point velocities. The AI techniques considered are the Backpropagation Neural Network (BPNN), Radial Basis Function Neural Network (RBFNN), Generalized Regression Neural Network (GRNN) and Group Method of Data Handling (GMDH).

2.3.1 Model Prediction Processes

The aim of the ANN was to find a solution to generalize a multidimensional input and output mapping challenges so that it does not predict beyond limits of the training data.

Pruning was done to allow for better performance of the models by taking away the outliers and noisy data, especially the white noises.
In all 1070 datasets were actualized for the eight CORS observed in weekly manner.
The dataset was divided into two (2) subsets: (i) for training and (ii) for testing which was not presented to the ANN during the training.
The training dataset was extensive and comprehensive and was representative enough for all possible variations on which the models were tested.
The models were able to determine the optimum value of the velocity rate for the geodetic points under study with a specific number of inputs layers and neurons for the processing.
All the models development based on these aforementioned techniques were carried out using MATLAB program.

2.3.2 Backpropagation neural network

The Backpropagation Neural Network (BPNN) is one of the widely used neural networks for prediction purposes. It has been widely used for the prediction of seismic activities such as earthquakes, tremors, tectonic movements, etc. Neural networks are named after simple processing units in the brain called neurons. (Amnieh *et al*., 2010; Saadat *et al*. 2014; Sawmliana *et al*., 2007; Monjezi *et al*., 2010b, Khandelwal *et al*., 2011). The BPNN is a feed forward neural network with input, hidden and output layer and each layer consist of neurons that are connected to neurons in the previous and next layers by connection weights (w_{ij}) as shown below in Figure 4.1.
BPNN is designed to accommodate multiple hidden layers. Within the layers, the input layer receives an external input vector associated with individual weights with a constant bias term. The weighted inputs are sent to the hidden layer. Inputs to each neuron in the hidden layer are transformed by a mathematical nonlinear activation function. Hyperbolic tangent sigmoid or logarithmic sigmoid is preferably used as the activation function (Dorofki *et al., 2012).*

In this study three (3) inputs were done i.e. V_x, V_y and V_z, 50 hidden layers with their synaptic weights and 1 output layer.
The output from the hidden layer Y_i, Equation (1) is then fed as input to the output layer. In the output layer, the input – output transformation is done by linear activation function to produce a final network output, Equation (2).

$$Y_i = f\left(\sum_{i=1}^{m}(w_{ij}\,X_j + b_i)\right) \tag{2}$$

where w_{ij} is the weight connecting the input layer to the hidden layer b_i, is the bias term and denotes the transfer function used in the hidden layer $f()$.
$\hat{y}=Y_i$

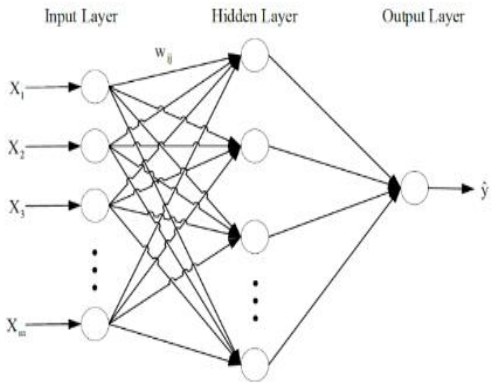

Figure 3. ***BPNN Architecture***

The selection of a suitable training method, transfer function, number of hidden layers, and number of neurons in the hidden layers is the most important step in creating a BPNN (Ziggah et al., 2016). As a universal approximator of any complicated issue, it has been demonstrated that a BPNN with one hidden layer is adequate (Hornik *et al.*, 1989; Ziggah *et al*., 2016). As a result, this research only employed one hidden layer.

The hyperbolic tangent was employed in this study as the transfer function for the hidden layer of the BPNN model, while the linear transfer function was used for the output layer. Levenberg-Marquardt (Hagan *et al*., 1996), Bayesian regularization (Foresee and Hagan, 1997), and the scaled conjugate gradient (Miller, 1993) were taken into account for the backpropagation training techniques. Based on an experimental procedure, the ideal number of hidden neurons was chosen for each of the training functions. In other words, for each training function, the number of hidden neurons that produced the highest correlation coefficient and the lowest mean squared error (MSE) for both the training and test data sets was chosen as the optimal number. The outcome of each training function was then compared with the architecture that was chosen.

The maximum number of iterations (number of epochs) is often set rather large since it is impossible to predict how many iterations will be needed until training is terminated (Hagan et al., 1996). Training is more reliable when the learning rate is modest. The training may not converge or even diverge if the learning rate is excessive. In some circumstances, the weight fluctuations may be so significant that the optimizer exceeds the minimum and exacerbates the loss (Surmenok, 2017). A large momentum coefficient can aid in accelerating the network's convergence rate. However, if the momentum coefficient is set too high, there is a chance that it will exceed the minimum, which might make the network unstable.

In addition to slowing network training, a momentum coefficient that is too low cannot dependably avoid local minima (Baughman and Liu, 2014). As a result, for prediction modeling in this study, 5000 epochs for the network that was trained, with a learning rate of 0.03, the minimum performance gradient to be 0.0000001, and a momentum coefficient of 0.7. Also for the network performance function evaluation the Mean Squared Error was used.

2.1.3 Radial basis function neural network

A feed-forward neural network with three layers—one input layer, one hidden layer, and an output layer—is known as a radial basis function neural network (RBFNN). Figure 4.2 shows

an example of a common RBFNN architecture with an input vector, Xi(X1, X2, X3,...,Xm), radial basis functions, weights, and output.
Without using weight connections, the input layer transmits inputs from the surrounding environment to the concealed layer. A radial basis function, which serves as the hidden layer's component for non-linear processing, is present in each neuron. Radial basis functions come in a variety of shapes and sizes (Shin and Park, 2000).
However, the Gaussian function (Singla *et al*., 2007), which is the radial basis function employed in this work, is the most popular. Only a small input space region where the Gaussian is centered affects how the Gaussian function behaves (Poulos *et al*., 2010). After that, each neuron calculates the Euclidean distance between each input item and the Gaussian function's center.
To implement the RBFNN effectively, appropriate centers for the Gaussian function must be found.
Two parameters, namely the center and width parameters, define the Gaussian function.
The Gaussian function is then updated with the obtained Euclidean norm to provide the results indicated in Equation (3).

$$net_j = exp\left(-\frac{\|X_i - c_j\|^2}{2\sigma_j^2}\right) \quad (3)$$

Where $\|X_i - c_j\|$ is the computed Euclidean distance between *Xi* and c_j. The input to the output layer is the weighted sum of the outputs of the hidden neurons. This is then processed by a linear function in the output layer to produce the final output, *ˆk y* of the RBFNN as expressed in Equation (4).

$$\hat{y}_K = b_0 + \sum_{j=1}^{r} w_{jk} net_j \quad (4)$$

where w_{jk} is the connection weight between the hidden layer and the output layer, b_0 is the bias term and *r* denote the number of hidden neurons.
The centres, width parameters and a set of weights are adjusted during the training process of RBFNN. This is done with objective function of minimizing the mean square error Equation (5) between the desired output d_k, and the predicted output, Y_k. (5)

$$Min\ (MSE) = \frac{1}{N} + \sum_{k=1}^{N} (d_k - \hat{y}_k)^2$$

where *N* is the number of observations.

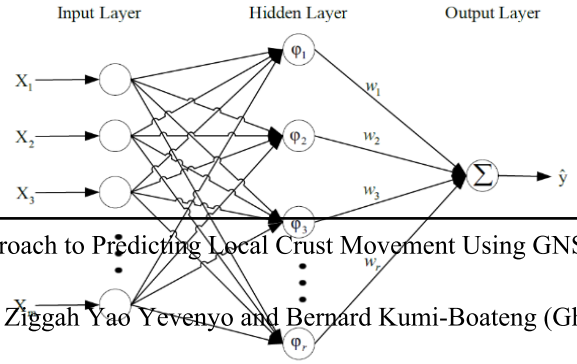

Figure 4. RBFNN Architecture

The RBFNN model was trained using the gradient descent learning algorithm in which the weights are adapted in part to the deviation between the predicted and target outputs. The adjustable parameters that affect the training of the RBFNN are the width parameter and the maximum number of neurons in the hidden layer. Width parameter values of 0.1 to 50 with a step size of 1 were investigated for both ground vibration and air overpressure models. The maximum numbers of neurons ranging from 1 to 40 were also investigated with an optimum spread constant of 12. In choosing the optimum RBFNN architecture, there was a bit of iterations for the width value and the maximum number of neurons in the hidden layer that gave the least MSE and largest correlation coefficient in both training and testing data set was selected.

2.3.4 Generalized regression neural network

The input layer, pattern layer, summation layer, and output layer make up the one pass learning network known as the Generalized Regression Neural Network (GRNN) (Figure 4.3). A feedforward connection is used to connect these levels. Information for input is received by the input layer and sent to the pattern layer. Euclidean distances between each input and each pattern that has been saved are determined at the pattern layer. Then, a nonlinear activation function receives these estimated distances as input. The output is then delivered to the summing layer. The S-summation neuron and the D-summation neuron make up the summation layer. The unweighted outputs of the pattern neurons are calculated by the D-summation neuron, while the S-summation neuron adds up the weighted outputs of the pattern layer.

Finally, as shown mathematically in Equation (6), the output layer produces the required estimate, y(x), by dividing the output of the S-summation neuron by the output of the D-summation neuron (Specht, 1991).

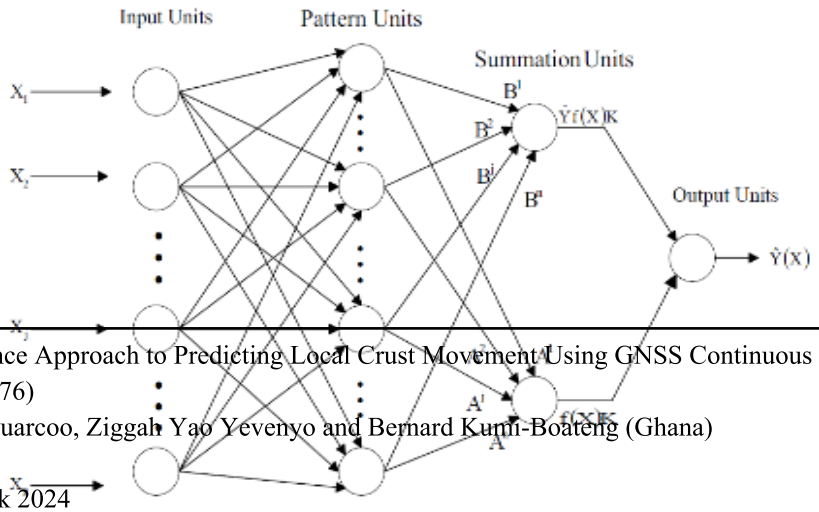

Figure 5. GRNN Architecture

$$Y(x) = \frac{\sum_{i=1}^{n} w_i k(x, x_i)}{\sum_{i=1}^{n} k(x, x_i)} \quad (6)$$

where *Y(x)* is the predicted value of input *x*, *wi* is the activation weight for the pattern layer neurons at *i* and $k(x, x_i)$ is the radial basis function kernel between input *x* and training samples, *xi*.
In the case of a Gaussian kernel, *k (x, xi)* is given in Equation (7) as:

$$k(x, x_i) = e^{\frac{-d^2}{2\sigma^2}} \quad (7)$$

where $d_i = \|x - x_i\|$ is the Euclidean distance between the training samples *xi* and the input *x* and σ is the spread parameter (Specht,1991).

In the GRNN the spread parameter is significant in selecting the optimum GRNN model which influences the precision of prediction, hence, the optimal spread constant input was 29 and 40 as the number of neurons. The parameter values of 0.1 to 1 with a step size of 0.01 were investigated and the value that gave the best correlation coefficient and lowest MSE for both training and testing data sets was chosen as the optimum model.

2.3.5 *Group method of data handling*

For modeling non-linear, unstructured, and complicated systems, Ivakhnenko (1970) created the Group Method of Data Handling (GMDH) approach, a form of feed-forward neural network (Mofki et al., 2018). The method uses a multilayer network made up of many quadratic neurons organized in a certain pattern to translate a collection of input variables into matching target variables. The best network topology may be chosen via GMDH by automatically learning the underlying, complicated relations that control the system variables. Due to its ability to generalize well and suit the complexity of non-linear systems with a relatively easy-to-use and numerically stable network, the GMDH is a useful tool.

The inductive self-organizing process utilized to create a multi-parametric model with workable variations is what distinguishes the GMDH technique from other approaches.
Equation (12) of the Kolmogorov- Gabor polynomial, a multilayer network of second order, is used by GMDH to characterize the intricate nonlinear interactions between the system's inputs and outputs (Assaleh *et al*., 2013).

$$\hat{y} = a_0 + a_1 x_i + a_2 x_j + a_3 x_i x_j + a_4 {x^2}_i + a_5 {x^2}_j \quad (8)$$

where $\hat{y}$ is the predicted output, *a* is the vector of the coefficient of the polynomial function, x_i and x_j are the input variables.

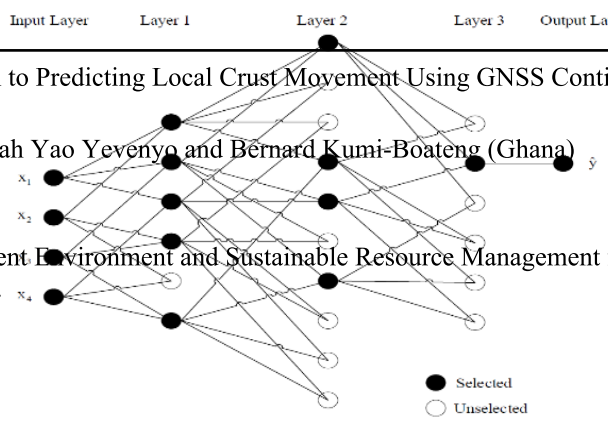

Figure 6: ***GMDH Architecture***

A GMDH architecture with five inputs and three layers and some selected and unselected neurons is shown in Figure 6.

2.4 Model Prediction Performance

The prediction accuracies of each of the predictive models for the Geodetic Point Velocities were analyzed using statistical performance indicators of Mean Square Error (MSE), Root Mean Square Error (RMSE), Mean Absolute Error (MAE) and Coefficient of determination (R^2).
The following equations (Equations 9-12) present their mathematical notations:

$$MSE = \frac{1}{n}\sum_{i=1}^{n}(o_i - p_i)^2 \tag{9}$$

$$RMSE = \sqrt{MSE} = \sqrt{\frac{1}{n}\sum_{i=1}^{n}(o_i - p_i)^2} \tag{10}$$

$$MAE = \frac{1}{n}\sum_{i=1}^{n}|O_I - p_i| \tag{11}$$

$$R^2 = \frac{(\sum_{i=1}^{n}(o_i - \bar{o})\,(p_i - \bar{p}))^2}{\sum_{i=1}^{n}(o_i - \bar{o})^2\, x\, (p_i - \bar{p})^2} \tag{12}$$

where *n* is the total number of test samples, *oi* are the observed values, *p* are the predicted $\overline{o}$ values is the mean of the observed values and is the mean of the predicted values $\overline{p}$.

An evaluation of the various prediction models was done by plotting the observed against the predicted with a 1:1 line, a 95% confidence interval (CI) (Equation (13)) and 95% prediction interval (PI) (Equation (14)).

$$PI = p_i \pm t_{(\alpha/2,n-2)} SD \sqrt{1 + \frac{1}{n} + \frac{(o_i - \bar{o})^2}{\sum(o_i - \bar{o})^2}} \quad (13)$$

$$CI = \bar{p} \pm Z_{\alpha/2} \frac{\sigma}{\sqrt{n}} \quad (14)$$

where $\overline{p}$ is the mean of the predicted values, σ is the population standard deviation, $Z_{\alpha/2}$ is the Z value for the desired confidence level α and n is the number of predicted values. At a 95% Confidence Interval, $Z_{\alpha/2}$ = 1.96.

$$s = \sqrt{\frac{\sum(O_i - P_i)^2}{n - 2}} \quad (15)$$

where n is the total number of samples, Oi are the observed PPV values, Pi are the predicted PPV values, $\bar{o}$ is the mean of the observed PPV values, $t_{(\alpha/2,n-2)}$ is the α-level quartile of a t-distribution with n – 2 degrees of freedom, SD is the standard deviation of the residuals.

3.0 Results and Discussion

3.1 AI Models used for the Prediction of Local Crust movement.

In this study the 4 (Four) ANN models where used to in the training and testing for the prediction of the local crust movements in the direction X, Y AND Z.
An optimum number of neurons were selected for the training. The data was divided into 2; One (80%) for the training and the second, (20%) for the testing of the prediction.
The training was done based on the components of the data obtained from the GAMIT/GLOBK processing, i.e. Velocity X, Y and Z(mm).

Table 2. BPNN Model Results

	Training				Testing			
Compt.	**RMSE**	**MAE**	**MSE**	R^2	**RMSE**	**MAE**	**MSE**	R^2
X	0.675233	0.491479	0.455939	0.069154	1.761623	0.464397	1.327261	0.004135
Y	0.669445	0.554065	0.448157	0.416752	1.024159	0.867661	1.048902	0.214994
Z	0.669445	0.012158	0.482209	0.427487	1.024159	1.075831	1.253964	0.298106

They were then evaluated using some statistical indicators like the Root Mean Square Error (RMSE), Mean Squared Error (MSE), Mean Absolute Error (MAE), and Coefficient of determination (R^2).

To assess the performance of the model, 20% of the dataset, representing 208 points were used. The geocentric Cartesian coordinates (X, Y, Z) for the 208 points with their respective velocities (V_X, V_Y and V_Z) were known. The predicted values of the crustal velocities from the models were subsequently compared with the actual observed values. The differences between the observed velocities and the predicted values were computed for each model. The differences were computed by

$$E_{(Model)} = V_{(observed)} - V_{(predicted)}$$

where $E_{(Model)}$ is the difference of the model being considered, $V_{(observed)}$ is the actual observations for velocities V_X, V_Y and V_Z and $V_{(predicted)}$ is the predicted model values for V_X, V_Y and V_Z.

In this study, the parameters for the training of the BPNN model were a bit iterative in order to yield the best results. The architecture for the training of the 'X' velocity component varies from that of the 'Y' and 'Z'. For the 'X', were three (3) inputs layers with fifty-three (53) neurons and one (1) output and an epoch of 5000. The training RMSE was 0.673599 and the testing RMSE was 1.330328.

The velocity 'Y' has an architecture of three (3) input layers, six (6) hidden neurons and one (1) output layer. The training RMSE was 0.666693 and a testing RMSE of 0.992875.

Table 3. The GMDH Model Results

	Training				Testing			
Compt.	**RMSE**	**MAE**	**MSE**	R^2	**RMSE**	**MAE**	**MSE**	R^2
X	0.699851	0.507695	0.489791	0.045868	1.223258	1.027360	1.327261	0.202089
Y	0.741993	0.597200	0.550555	0.318363	0.842400	0.694023	0.709637	4.10E-05
Z	0.917724	0.668461	0.842218	0.064061	0.951927	0.894408	0.906165	4.35E-01

For the velocity 'Z', though same as the 'Y', with three (3) input layers, six (6) hidden neurons and one (1) output layer had a training RMSE of 0.674554 and a testing RMSE of 0.989783.
A table 5.1, 5.2, 5.3 and 5.5 shows the results of the various models during the training and testing. It indicates the RMSE, MAE, MSE ANS the R^2 of the three (3) velocity components, V_X, V_Y and V_Z during the training and testing from the models.

3.1.1 Results

Backpropagation Neural Network Architecture

The BPNN architecture used for this research consisted of three (3) layers, namely: the input layer, hidden layer and output layer. It is made up of five inputs with a hyperbolic tangent hidden layer transfer function and a linear output layer transfer function. The network was trained for 5000 epochs using the Bayesian Regularization Backpropagation algorithm with a learning rate of 0.05 and a momentum coefficient of 0.7. The optimum structure of the BPNN was [3 – 53 – 1] that is three inputs, fifty-three hidden neurons and one output.

The RMSE of the BPNN is within the ranges of 0.669 to 0.675 for all three components Vx, Vy and Vz during the training but yielded the highest during the testing, ranging from 1.024 to 1.762.
It has the lowest coefficient of determination (R^2) during the testing of the Vx component compared to the other statistical evaluators.
The Mean Absolute Error also yielded the least value during the training, i.e. a value of 0.0122 and also produced values from 0.867 to 1.076 during the testing for all three components.

GMDH Neural Networks

The GMDH model with the lowest MSE and highest R value was found to have three parameters in input layer, two hidden layers with three neurons and a single value as model target as output layer. The corresponding parametres for the GMDH for Geodetic Point Velocity prediction are shown in below:
Table 3 shows the optimal training and testing results for the GMDH technique based on the 4 statistical evaluators used; RMSE ,MAE, MSE AND $R^{2.}$

In table 5.3 it can be noticed that the RMSE FOR THE GRNN training of all 3 variables were in the ranges of 0.655912 to 0.652352 but the Vz component in the prediction RMSE was 1.599513. The R^2 which was the least of all is the ranges of 0.128551 to 0.361591 with a MSE difference of 0.01 in all 3 variables.
The RMSE of the Vz for the GRNN testing was 1.599513, approximately 0.61 differences from the Vx and Vy.
The R^2 were good for both the training and testing. The difference in result ranges from 0.00 to 0.20

Table 4. The RBFNN Model Results

			Training			Testing		
Compt	**RMSE**	**MAE**	**MSE**	R^2	**RMSE**	**MAE**	**MSE**	R^2
X	0.65591	0.46439	0.42684	0.128551	0.98862	0.97760	1.617353	0.000897
Y	0.65591	0.53455	0.43022	0.440096	0.98862	0.80074	0.982079	0.124335
Z	0.65235	0.47778	0.42293	0.361591	1.59951	1.44409	2.570742	0.324179

For the RBFNN model for geodetic point velocity prediction, the width parameter value and the maximum number of neurons that gave the highest R^2 and the lowest MSE was 0.324179 and 0.43022061, respectively.
Hence, the optimum RBFNN architecture selected for predicting geodetic point velocity has three inputs with forty hidden layer of neurons and one output layer, that is, [3–40–1]. Table 5.4 presents the training and testing results based on the RMSE, MAE, MSE and R^2 criteria.

From Tables 5.1, 5.2, 5.3 and 5.4, it can be observed that, the various RBFNN and GRNN models have very close R^2 values in the range, 0.00034 to 0.4439 and MSE values within the ranges 0.0005 to 1. 2520.
These results confirm that the some of the models accurately predicted geodetic point velocities in some components, i.e. to say, some models were able to train and predict some specific components with high accuracy. For instance, looking at Table 5.3, the GRNN was good in predicting all three variables, Vx, Vy and Vz. Whereas the GMDH was only able to predict the Vx with high accuracy as compared to the other variables it predicted.
This study assessed the capability AI techniques of BPNN, GMDH, RBFNN and GRNN as alternate predictive tool for Geodetic Point Velocity. The purpose was to determine whether those proposed these AI techniques could predict comparable and satisfactory geodetic point velocities. Considering the dimensioned error statistic indicators (MSE, RMSE, R^2 and MAE), it was found that no AI technique actually produced the least MSE, RMSE R^2 and MSE for all 3 components. Some models were good in training and predicting some components of velocities with high accuracies.
The GRNN was the best among all the candidate models in terms of predicting the values for the Vx component of the training and testing.

This was however, closely followed by the GRNN and RBFNN approach. These results indicate that comparatively, the GRNN was able to learn well and was able to predict the Vy components. And the RBFNN was good to produce the least values for the Vy components during the training and predictions.
This is in line with the rule of thumb that, the closer the values of MSE, RMSE R^2 and MAE are to zero, the better the prediction capability of the model.

Table 5. The GRNN Model Results

	Training				**Testing**			
Compt.	**RMSE**	**MAE**	**MSE**	R^2	**RMSE**	**MAE**	**MSE**	R^2
X	0.655912	0.464397	0.000334	0.128551	0.988625	0.977609	0.855997	0.000897
Y	0.655912	0.534559	0.534559	0.440096	0.892702	0.800749	0.796918	0.124335
Z	0.652352	0.477789	0.534559	0.361591	0.791420	1.4440930	0.626345	0.324179

However, a careful study of Table 5 indicates that comparatively, the GMDH technique was better, and it performed fairly well because its MSE, RMSE, R^2 and MAE results deviated only marginally as compared to the other models considered in this research. Undoubtedly, it can be stated that GMDH ANN model can yield a very comparable and closely related geodetic point velocity prediction results. In comparison to the other candidate models, the GMDH model outperformed the rest. On the contrary, the BPNN model was able to learn and generalize well during the training but could not produce acceptable results across the entire testing dataset. A pictorial view of the predictive strength of the models can additionally be viewed in Figures 5.2, 5.3, 5.4 and 5.5. The R^2 results presented in Table 5.1, 5.2, 5.3 and 5.4 provide quantitative evidence on how dependent the predicted geodetic point velocity values are from the actual observations. With reference to Table 5.1, it can be seen that the BPNN had high RMSE and MSE values during the training than the testing. This means that the model performed well in the sample but has little predictive value when tested out of the sample. However, it can be observed that the RBFNN results for Vz had the highest R^2 value of 0.324179. The other models (BPNN, GMDH and GRNN) could produce comparable results as their R^2 values were marginally different from that of the GMDH model which ranges between the ranges of 0.002 to 0.298.

Based on the results obtained it was found out that the GMDH model outperformed the rest of the models followed by the GRNN which produced comparable and satisfactory results. Hence GMDH technique is proposed to be suitable tool to predict geodetic point velocities. The RMSE, MSE, MAE and R^2 statistical techniques were used as a models performance tool to appraise the models. They were used in this study to analyze the results of the predictions

and to select the best model among the candidate models applied. When these techniques are applied, the best results starts from 0 to infinity with 0 being the best value, hence the model with that smallest value is the preferred model. The resultant values (Table 5.1, 5.2, 5.3 and 5.4) showed that the GMDH model had a better capability of producing reliable results than the other investigated models. This is because, among the methods, the GMDH had the least statistical values (Table 5.1, 5.2, 5.3 and 5.4) and thus was selected as the best technique over the other AI methods. The obtained results also revealed that the other AI models (RBFNN, GRNN and BPNN) produced comparable and satisfactory prediction results in some components of the geodetic point velocities. This affirms the assertion made that; the other AI models can suitably be used to predict geodetic point velocities.
Therefore, on the basis of these statistical analyses presented in this study, it can be stated categorically that the potential of AI models in predicting geodetic point velocities for the southern part of Ghana has been duly investigated.

4.0 CONCLUSIONS AND RECOMMENDATIONS

4.1 CONCLUSION

Under investigation in this study is the prediction of Geodetic Point Velocities in the southern part of Ghana using four (4) AI techniques. In this case four models AI techniques of GRNN, RBFNN, GMDH and BPNN have been proposed and tested as alternative tool that can be adapted for prediction of Geodetic Point Velocities. To provide a comprehensive performance evaluation of these techniques, four statistical evaluation methods namely RMSE, MAE, MSE and R^2 were used to access the suitability of the proposed models. To achieve this aim, a total of 1070 RINEX3.0 format data points were acquired from LISAG CORS with their velocities. These data sets were then processed using Trimble Geomatic Office for their natural coordinates and onward processing with GAMIT/GLOBK to derive their respective station velocities. The data were then used to run the various predictive models in MATLAB.

The 1070 points were then dived into 2 datasets, 80% and 20%; 80% for training and the remaining 20% for the independent testing of the model.
To run the AI models, the number of points, velocities Vx, Vy and Vz with their respective coordinates Xm, Ym and Zm were used as the input parameters while the geodetic point velocity values were used as the output parameter. Statistical performance criteria of Mean Square Error (MSE), Root Mean Square Error (RMSE), Mean Absolute Error (MAE) and Coefficient of determination (R^2) were used as the basis for evaluating the performance of the techniques employed in this study. These statistical approaches were used to in selecting the best model among the candidate models in this study.

Based on the statistical results obtained, it was found out that three out of the four proposed AI techniques (GRNN, RBFNN, BPNN and GMDH) could produce sound geodetic point velocity predictions. Hence the GMDH was proposed to be used as suitable to predict

geodetic point velocity. This was selected based on the statistical approach for the evaluation of the prediction of the geodetic point velocities.
Therefore, the GMDH model could be used as a means of forecasting geodetic point velocities and can be applied in the field of geodesy or related fields were GPV is needed to understanding the issues of the earth and its seismicity.
To this end, it is clear that the computational adaptive strategy of the AI techniques applied in this research enabled the correct calibration and generalization to the data set.

4.2 Recommendations

From results obtained from this project, it is recommended that:

i. These AI techniques in predicting GPV should be adopted by Geoscientists in forecasting seismic activities of the earth and its related fields where applicable. ***This is in line with the Sustainable Development Goal Eleven (11) which aims at making cities and human settlements inclusive, safe, resilient and sustainable.***
ii. A research is taken to cover the whole of the country or continent to determine the extent of crust movement by increasing the number of CORS.
iii. Different datasets be utilized to evaluate the influence of point density on the geodetic point velocity prediction outcomes. In this project, the candidate models provided reasonable predictions, so it can be an alternative tool for predicting the geodetic point velocities.
iv. The prediction of accurate local Geodetic Point Velocities needs to be further researched and discussed. A hybrid model of these when researched, will not be farfetched to determine its contribution to the accuracy factor when predicting.

REFERENCES

Amnieh, H.B., Mozdianfard, M.R. and Siamaki, A. (2010) "Predicting of blasting vibrations in Sarcheshmeh copper mine by neural network", Safety Science, No. 48, Vol. 3, pp.319-325.

Baughman, D. R., & Liu, Y. A. (2014), "Neural networks in bioprocessing and chemical engineering", Academic press.

Biological and Environmental Engineering, No. 33, Vol. 5, pp.39-44.

Cakir, L., and Yilmaz, N. (2014), "Polynomials, radial basis functions and multilayer perceptron neural network methods in local geoid determination with GPS/levelling," Measurement, Vol.57, pp. 148–153.

Dorofki, M., Elshafie, A. H., Jaafar, O., Karim, O. A. and Mastura, S. (2012), "Comparison of artificial neural network transfer functions abilities to simulate extreme runoff data", International Proceedings of Chemical,

Foresee, F.D. and Hagan, M.T. (1997), "Gauss-Newton approximation to Bayesian learning", In Proceedings of international conference on neural networks, Vol. 3, pp. 1930-1935.

Hagan, M.T., Demuth, H. B. and Jesús, O. D. (2002), "An introduction to the use of neural networks in control systems", International Journal of Robust and Nonlinear Control: IFAC-Affiliated Journal, No. 12, Vol. 11, pp.959-985.

Hornik, K., Stinchcombe, M., and White, H. (1989), "Multilayer feedforward networks are universal approximators", Neural networks, No. 2, Vol. 5, pp. 359–366.
Khandelwal, M., Lalit Kumar, D. and Yellishetty, M. (2011), "Application of soft computing to predict blast-induced ground vibration", Engineering with Computers, No. 27, Vol. 2, pp. 117 – 125.
Monjezi, M., Bahrami, A. and Varjani, A.Y., (2010), "Simultaneous prediction of fragmentation and flyrock in blasting operation using artificial neural networks", International journal of rock mechanics and mining sciences, No. 47, Vol. 3, pp. 476-480.
Poku-Gyamfi, Y. (2009), "Establishment of GPS Reference Network in Ghana", PhD Dissertation, Universitat der Bundeswehr Munchen, Germany, pp. 1-177.

Sawmliana, C., Roy, P. P., Singh, R. K. and Singh, T. N. (2007), "Blast induced air overpressure and its prediction using artificial neural network", Mining Technology, No. 116, Vol. 2, pp.41-48.

Saadat, M., Khandelwal, M. and Monjezi, M. (2014.) "An ANN-based approach to predict blast-induced ground vibration of Gol-E-Gohar iron ore mine", Iran, Journal of Rock Mechanics and Geotechnical Engineering, No. 6, Vol. 1, pp.67-76.

Surmenok, P. (2017), "Estimating an optimal learning rate for a deep neural network", Towards Data Science, No. 3, Vol. 5, pp.6-16.

Ziggah, Y.Y., Youjian, H., Tierra, A., Konate, A.A. and Hui, Z. (2016), "Performance evaluation of artificial neural networks for planimetric coordinate transformation—a case study, Ghana", Arabian Journal of Geosciences, Vol. 9, No. 17, pp. 1-16.

Ziggah, Y.Y., Yakubu, I. and Kumi-Boateng, B. (2016), "Analysis of Methods for Ellipsoidal Height Estimation – The Case of a Local Geodetic Reference Network", Ghana Mining Journal, Vol. 16, No. 2, pp. 1 - 9.

Ziggah, Y. Y., Youjian, H., Yakubu, I. and Laari, P.B. (2019), "Least Squares Support Vector Machine Model for Coordinate transformation", Geodesy and Cartography, Vol. 45, No. 1, pp. 16-27.

Author

C. K. Quarcoo is a Geomatic Engineer and a staff of the Survey and Mapping Division of the Lands Commission, Ghana. He holds a Diploma in Land Surveying from Aqua Foundation-Delhi, BSc. Geomatic Engineering from KAAF University College, MSc. Land Policy and Administration from the University of Cape Coast and currently a Mphil. Geomatic Engineering

student of the University of Mines and Technology, Tarkwa. He is a member of Ghana Institution of Surveyors, Ghana Institution of Engineers and Association of Building Technicians, Ghana. His research works covers the application of artificial intelligence in Land surveying and seismicity of the earth. He has done quiet an extensive works in Land surveying which are but not limited to Engineering surveying, Cadastral surveying, mapping and other cartographic works of high repute.

CONTACTS

Surv. Ing. Christian Kartey Quarcoo
Survey and Mapping Division
Lands Commission
P.O. Box CC42,
Cape Coast
GHANA
Tel. +233207312814
Email: phartcat@yahoo.com
Web site: www.lc.gov.gh